ChemComm

RSC Publishing

COMMUNICATION

View Article Online
View Journal | View Issue

Controlled synthesis of non-epitaxially grown Pd@Ag core–shell nanocrystals of interesting optical performance†‡

Cite this: *Chem. Commun.*, 2013, **49**, 4379

Received 29th October 2012,
Accepted 2nd December 2012

DOI: 10.1039/c2cc37825f

www.rsc.org/chemcomm

Jianxiao Gong,[a] Fei Zhou,[b] Zhiyuan Li*[c] and Zhiyong Tang*[a]

Pd@Ag core–shell nanocrystals are synthesized through a seed mediated method. Ag shells are found to be grown in a non-epitaxial growth manner, with lots of defects to release the strain originating from lattice mismatch.

Owing to their fantastic optical and catalytic properties, controllable synthesis of noble metal nanocrystals (NCs) has been extensively studied.[1,2] Recently, research interests have been switched from single to binary and multiple elements, leading to integration of Au, Ag, Pd and Pt into the same structures such as in core–shell NCs.[3] Unfortunately, a prerequisite to formation of most noble metal core–shell NCs is lattice matching between the core and shell element, allowing the epitaxial growth of another single crystalline shell onto the single-crystalline core.[4] This structural feature dramatically limits the available types of noble metal core–shell NCs. For instance, reports on the synthesis of Pd@Ag core–shell NCs is scare due to the large lattice mismatch (cell parameter: Pd 3.891 Å, Ag 4.086 Å; lattice mismatch: 5.012%).[5]

Herein, we explore that Pd@Ag core–shell NCs can be fabricated *via* a non-epitaxial growth mode of Ag shells onto Pd cores. Although with a uniform cubic shape, the Ag shells do not have perfect single crystalline structure and contain lots of defects at the boundary with Pd cores, some of which extend to the surface of the Ag shells. The defects are the key to release the stress induced by the lattice mismatch. The localized surface plasmon resonance (LSPR) properties of such Pd@Ag core–shell NCs are investigated and compared with theoretical results.

Single-crystalline Pd nanocubes enclosed with six {100} facets of side length 18 ± 3 nm (Fig. S1‡), are chosen as seeds.[6] Cetyltrimethylammonium chloride (CTAC) is used as the surfactant to mix with the growth solution containing $AgNO_3$ and L-ascorbic acid, giving rise to production of Pd@Ag core–shell NCs.[3b,f,7] As shown in Fig. 1, the sizes of NCs grow from ~18 to ~40 nm, indicating the formation of Ag shells. The Pd@Ag core–shell NCs of uniform sizes and shapes can spontaneously organize into ordered structures on silica substrates (Fig. 1A). Transmission electron microscopy (TEM) observation on single core–shell NCs clearly presents Moiré patterns (the patterns formed due to superposition of misfit of the two lattices) (Fig. 1C and Fig. S2‡), also suggesting the formation of Ag shells. Interestingly, these Moiré patterns are not straight and parallel. This is the first evidence of the incoherent overgrowth between the cores and the shells: (1) the curved Moiré patterns imply the possible existence of defects. (2) When misfit lattices overlap each other in parallel, the Moiré patterns should also appear in

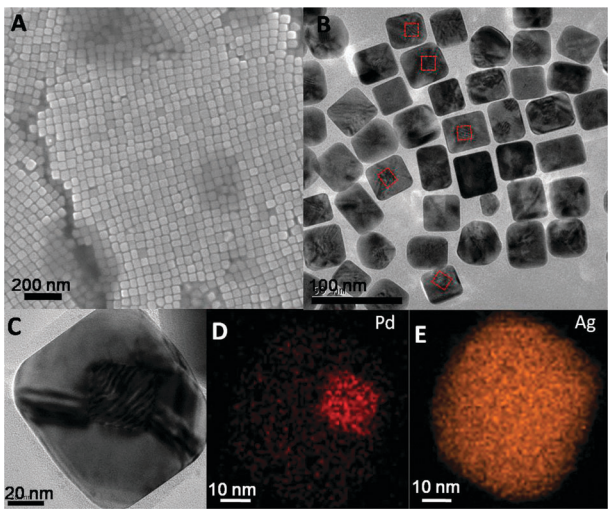

Fig. 1 (A) Scanning electron microscopy (SEM) images, (B, C) transmission electron microscopy (TEM) images and (D, E) element analysis mapping of Pd@Ag core–shell NCs.

[a] *Laboratory for Nanomaterials, National Center for Nanoscience and Technology, 100190 Beijing, China. E-mail: zytang@nanoctr.cn; Fax: +86-10-62656765; Tel: +86-10-82545580*

[b] *Key Laboratory of Materials Physics, Anhui Key Laboratory of Nanomaterials and Nanotechnology, Institute of Solid State Physics, Chinese Academy of Sciences, Hefei 230031, Anhui, China*

[c] *Laboratory of Optical Physics, Institute of Physics, Chinese Academy of Sciences, Beijing 100190, China*

† This article is part of the *ChemComm* 'Emerging Investigators 2013' themed issue.

‡ Electronic supplementary information (ESI) available: Methods; SEM, TEM, HRTEM images for Pd seeds; UV-vis spectrum of Pd seeds; illustration of the growth mechanism. See DOI: 10.1039/c2cc37825f

parallel. The non-parallel patterns demonstrate possible shifting or rotation of the two lattices.

It is obvious that Pd cores are not located at the center of the NCs (Fig. 1D and E, Fig. S2‡). Similar asymmetric Pd@Ag nanostructures have been obtained and they are attributed to the anisotropic growth speed of Ag atoms on the Pd cores.[5] Nevertheless, in that report the deposition of Ag atoms also follows the epitaxial growth on one/three/six sides of the Pd cubic seeds, leading to the products of the structures in which the facets of Ag shells are parallel to the facets of Pd seeds (cubes are enclosed with {100} facets for noble-metal NCs of face-centered cubic lattice). On the contrary, the Pd@Ag core–shell NCs synthesized in our work are quite different: the facets of the cores (enclosed by red dotted squares in Fig. 1B and Fig. S2‡) and the shells (enclosed by blue dotted squares in Fig. S2‡) are not always parallel and appear randomly with a small included angle. The non-parallel relationship between the core and the shell facets provides the second evidence on the non-epitaxial growth.

In order to examine the detailed structures of the Pd@Ag core–shell NCs, the individual NCs before and after coating with Ag shells are characterized by high-resolution TEM (HRTEM).

As shown in Fig. S3‡, the lattice of single-crystalline Pd seeds is clearly discerned with the incident electron beam direction along [100]. Fig. 2A represents a typical HRTEM image of Pd@Ag core–shell NCs. The position of the core is first identified through Moiré patterns (enclosed by red dotted square). A prominent structural feature of the Pd@Ag core–shell NCs is that though the lattice plane distance of 0.204 nm corresponding to that of Ag {200} planes ($d_{Ag\{200\}}$ = 0.2044 nm) can be distinguished, there are many defects existing especially near the boundary of the Pd core and Ag shell, and these defects extend through the Ag shell (white circles in Fig. 2A). The inset image of Fig. 2A represents the corresponding fast Fourier transform (FFT) image, which exhibits two series of diffraction patterns: one belongs to the regular spots of Ag with the incident direction along [100] (marked with red dots) and the other is of spots distributed irregularly. These additional and unassigned diffraction spots should originate from lattice distortion or defects. To observe these defects clearly, the magnified image of the boundary of the Pd core and the Ag shell (blue rectangular area in Fig. 2A) is shown in Fig. 2B. Four areas that are marked by 1 and 2 disclose two types of typical defects: (1) edge dislocation (ED): an inserting plane, in which the inserting atoms are marked by green, can be clearly seen in area 1. (2) Stacking fault (SF): the obvious distortion of the atoms' position, which originates from the gliding of the stacking fault planes along [110] direction, can be observed in area 2. The green circles in area 2 highlight these planes. It has been reported that in Au@Pd bimetallic alloy nanostructures, the strain between the surface Pd and the Au core is released by Shockley partial dislocations accompanied with SFs.[8] As for the Pd@Ag core–shell NCs, ED and SF are the main strain release mechanisms.

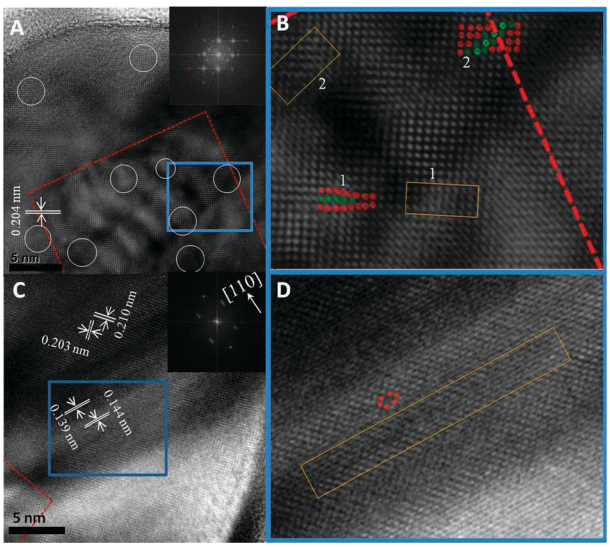

Fig. 2 (A) and (C): HRTEM images of Pd@Ag core–shell NCs (insets are FFT images). (B) and (D): magnified area enclosed with blue squares in (A) and (C), respectively. The red dotted lines in the images outline the core positions. The areas marked by yellow squares are areas with defects or dislocations. The red circles in (B) represent the regular atoms, while the green ones are the dislocation positions.

Fig. 2C and D represent another typical example of the Pd@Ag core–shell NCs. In Fig. 2C, the measured lattice parameters of four positions can be classified into two types of crystal planes: (1) 0.210 and 0.203 nm: the two planes in the perpendicular arrangement both correspond to the {200} planes of Ag with an obvious distortion along one direction expanded and another direction slightly compressed ($d_{Ag\{200\}}$ = 0.2044 nm); (2) 0.139 and 0.144 nm: the two planes in the parallel arrangement both correspond to the {220} plane of Ag ($d_{Ag\{220\}}$ = 0.1445 nm). Evidently, compression of the lattice appears along the [110] direction. In Fig. 2D, such type of distortion (the area enclosed by orange square) is labeled, combining with a few atom vacancies (the position surrounded by red circles). The presence of a large amount of defects and lattice distortion should be responsible for the abnormal Moiré patterns and the non-parallel arrangement of the core and the shell planes.

How do the Ag shells grow on the Pd cores to form the monodisperse cubic NCs? Generally, heterogeneous film growth follows three classic modes (Fig. S4A‡)[9]: (1) Frank–van der Merwe mode: layer-by-layer epitaxial growth for the case of perfect lattice match or slight mismatch with high interfacial bond energies and low supersaturation; (2) Volmer–Weber mode: island growth mode for the case of large mismatch under supersaturation to form three-dimensional nucleation; (3) Stranski–Krastanow mode: layer formation following island growth at medium lattice mismatch. Specific to growth of the noble metal core–shell NCs, the core offers nucleation sites and subsequent deposition of shell materials is determined by the lattice mismatch and the bonding energy between shell and core atoms. In the case of a lattice mismatch no larger than 3%, a uniform single crystal shell can be normally grown epitaxially on the core by the Frank–van der Merwe mode. When the mismatch is larger than 3%, nanoislands rather than a complete shell is formed on the surface of the core, as governed by the Volmer–Weber mode. In our system, the rather large lattice mismatch, 5.012%, limits the epitaxial growth of an Ag shell onto the Pd core (Frank–van der Merwe mode). However, formation of the complete Ag shells instead of discrete islands on the Pd cores demonstrates that the growth of Pd@Ag core–shell NCs does not follow the conventional Volmer–Weber or Stranski–Krastanow mode.

Here we suggest a novel formation mechanism of Pd@Ag core–shell NCs as follows (Fig. S4B‡): when $AgNO_3$ and AA are added into the solution of Pd seeds in the presence of CTAC,

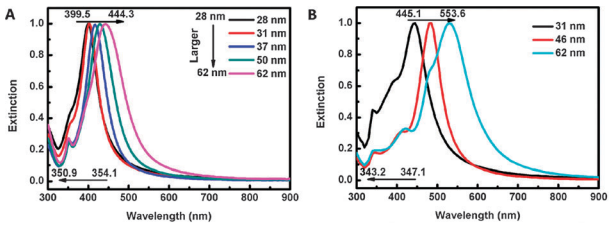

Fig. 3 (A) Experimental and (B) calculated UV-vis spectra of Pd@Ag core–shell NCs.

the $AgNO_3$ can be reduced to Ag atoms, which are deposited onto the surface of the Pd seeds initially in a layered mode. Owing to the 5.012% lattice mismatch between the Pd core and Ag shell, the strain accumulates after a few layers. Different from classic film growth (Fig. S4A‡), large surface energy and small surface area of NCs, in combination with the sufficient supply of Ag atoms, causes quick atom migration and fast formation of the shell. This process eliminates island formation, resulting in stress release through generation of defects in the shell. The production of the defects (mainly SF and ED, as shown by yellow dotted squares in Fig. S4B‡), gives rise to variation of the growth direction of the shell, eventually resulting in the formation of the Ag shells with different orientation compared with the cores. In addition, the ability of the CTAC surfactants in stabilizing {100} facets of Ag leads to formation of core–shell products of cubic shapes.[3b] The uncertain included angles between the Ag facets and the Pd seeds reveal variation of the growth direction, which should be attributed to the fast growth process of Ag shells and the existence of the defects. It should be noted that if a similar synthetic process is performed changing Pd seeds to Au seeds, Au@Ag core–shell NCs of perfect single crystalline shells and the symmetric structures are obtained (Fig. S5‡).[3f] Since the lattice parameters of Au and Ag are very similar (Au: 4.079 Å, Ag: 4.086 Å, mismatch: 0.17%), this experiment reveals the role of the lattice mismatch in generation of the non-epitaxial and asymmetric core–shell NCs.

By controlling the adding amount of the Pd seeds with size of around 18 nm, the overall sizes of the Pd@Ag core–shell NCs can be tuned between 28–62 nm (insert of Fig. 3A), which provides excellent candidates to study the optical properties of noble metal core–shell NCs of large lattice mismatch. Analogously to previous studies, the pure Pd seeds have no obvious LSPR peak in the UV-visible region (inset of Fig. S1‡).[6] For the Pd@Ag core–shell NCs there are two main peaks (Fig. 3A): one at 350–354 nm, almost independent of size, and the other at 399–444 nm with a remarkable bathochromic shift from 28 to 62 nm. Moreover, an absorption shoulder between these two peaks emerges as the size of the NCs increases, for instance, an absorption shoulder at around 400 nm is observed for the 62 nm Pd@Ag core–shell NCs (pink curve in Fig. 3A). To understand the LSPR of the Pd@Ag core–shell NCs, theoretical calculations were carried out using the discrete dipole approximation (DDA) method (Fig. 3B and Fig. S6‡). Because it is hard to evaluate the exact amount and the position of defects, our theoretical calculation was only based on the ideal core–shell model. Nevertheless, similarly to experimental results, with the NC sizes increasing, the calculated peaks at 343–347 nm corresponding to the multipole mode (Fig. S6‡) show a slight blue shift, while the calculated main peaks at 445–534 nm corresponding to the dipole mode (Fig. S6‡) exhibit a large bathochromic shift (Fig. 3B). We also note that though the change tendency is similar, both the shapes and positions of the absorbance peaks are quite different between experimental results (Fig. 3A) and theoretical calculation (Fig. 3B). The big difference in the calculated and experimental results highlights the effect of non-epitaxially grown core–shell structures on the optical performance of NCs, which should be attributed to the presence of defects and strain in the shells, and other factors such as the size and shape of Ag shells and electron transfer between Pd and Ag (Fig. S7‡).

In conclusion, we have developed a novel synthetic method to obtain Pd@Ag core–shell NCs of large lattice mismatching. ED and SF as the main strain release mechanisms are found to be responsible for the non-epitaxial growth of Ag shells onto the Pd cores. Furthermore, such core–shell nanostructures display unique optical properties different from conventional core–shell NCs with good lattice matching. This work can be expected to open the door towards the production of different types of noble metal core–shell NCs of large lattice mismatching, which will have great application potential in optics, catalysis and biology.

This work was supported financially by National Natural Science Foundation for Distinguished Youth Scholars of China (21025310, Z.Y.T.), National Natural Science Foundation of China (21003026, Y.G.; 20973047 and 91027011, Z.Y.T.), National Research Fund for Fundamental Key Project (2009CB930401, Z.Y.T.; 2013CB632704, Z.Y.L.).

Notes and references

1 (*a*) M. Rycenga, C. M. Cobley, J. Zeng, W. Li, C. H. Moran, Q. Zhang, D. Qin and Y. Xia, *Chem. Rev.*, 2011, **111**, 3669; (*b*) T. K. Sau and A. L. Rogach, *Adv. Mater.*, 2010, **22**, 1781; (*c*) A. R. Tao, S. Habas and P. Yang, *Small*, 2008, **4**, 310; (*d*) H. M. Chen and R.-S. Liu, *J. Phys. Chem. C*, 2011, **115**, 3513.
2 (*a*) W. Cheng, S. Dong and E. Wang, *Langmuir*, 2003, **19**, 9434; (*b*) W. Cheng, M. J. Campolongo, J. J. Cha, S. J. Tan, C. C. Umbach, D. A. Muller and D. Luo, *Nat. Mater.*, 2009, **8**, 519; (*c*) W. Niu, S. Zheng, D. Wang, X. Liu, H. Li, S. Han, J. Chen, Z. Tang and G. Xu, *J. Am. Chem. Soc.*, 2009, **131**, 697; (*d*) K. A. Willets and R. P. Van Duyne, *Annu. Rev. Phys. Chem.*, 2007, **58**, 267; (*e*) A. Tao, P. Sinsermsuksakul and P. Yang, *Angew. Chem., Int. Ed.*, 2006, **45**, 4597; (*f*) E. González, J. Arbiol and V. F. Puntes, *Science*, 2011, **334**, 1377; (*g*) J. Zhang, K. Sasaki, E. Sutter and R. R. Adzic, *Science*, 2007, **315**, 220; (*h*) N. Tian, Z.-Y. Zhou, S.-G. Sun, Y. Ding and Z. L. Wang, *Science*, 2007, **316**, 732; (*i*) J. He, P. Zhang, J. Gong and Z. Nie, *Chem. Commun.*, 2012, **48**, 7344.
3 (*a*) S. E. Habas, H. Lee, V. Radmilovic, G. A. Somorjai and P. Yang, *Nat. Mater.*, 2007, **6**, 692; (*b*) Y. Ma, W. Li, E. C. Cho, Z. Li, T. Yu, J. Zeng, Z. Xie and Y. Xia, *ACS Nano*, 2010, **4**, 6725; (*c*) H. Yoo, J. E. Millstone, S. Li, J.-W. Jang, W. Wei, J. Wu, G. C. Schatz and C. A. Mirkin, *Nano Lett.*, 2009, **9**, 3038; (*d*) C.-L. Lu, K. S. Prasad, H.-L. Wu, J.-a. A. Ho and M. H. Huang, *J. Am. Chem. Soc.*, 2010, **132**, 14546; (*e*) F.-R. Fan, D.-Y. Liu, Y.-F. Wu, S. Duan, Z.-X. Xie, Z.-Y. Jiang and Z.-Q. Tian, *J. Am. Chem. Soc.*, 2008, **130**, 6949; (*f*) J. Gong, F. Zhou, Z. Li and Z. Tang, *Langmuir*, 2012, **28**, 8959; (*g*) S. Xing, Y. Feng, Y. Y. Tay, T. Chen, J. Xu, M. Pan, J. He, H. H. Hng, Q. Yan and H. Chen, *J. Am. Chem. Soc.*, 2010, **132**, 9537.
4 J. Zhang, Y. Tang, K. Lee and M. Ouyang, *Science*, 2010, **327**, 1634.
5 (*a*) J. Zeng, C. Zhu, J. Tao, M. Jin, H. Zhang, Z.-Y. Li, Y. Zhu and Y. Xia, *Angew. Chem., Int. Ed.*, 2012, **51**, 2354; (*b*) C. Zhu, J. Zeng, J. Tao, M. C. Johnson, I. Schmidt-Krey, L. Blubaugh, Y. Zhu, Z. Gu and Y. Xia, *J. Am. Chem. Soc.*, 2012, **134**, 15822.
6 W. Niu, L. Zhang and G. Xu, *ACS Nano*, 2010, **4**, 1987.
7 E. C. Cho, P. H. C. Camargo and Y. Xia, *Adv. Mater.*, 2010, **22**, 744.
8 Y. Ding, F. Fan, Z. Tian and Z. L. Wang, *J. Am. Chem. Soc.*, 2010, **132**, 12480.
9 (*a*) M. Casavola, R. Buonsanti, G. Caputo and P. D. Cozzoli, *Eur. J. Inorg. Chem.*, 2008, 837; (*b*) L. Carbone and P. D. Cozzoli, *Nano Today*, 2010, **5**, 449.